Electronic structures and spin gapless semiconductors in BN nanoribbons with vacancies

Yanfei Pan[1] and Zhongqin Yang[1,2,*]
[1]*State Key Laboratory of Surface Physics and Department of Physics, Fudan University, Shanghai 200433, China*
[2]*Department of Chemistry, Northwestern University, Evanston, Illinois 60208, USA*
(Received 31 May 2010; revised manuscript received 7 September 2010; published 5 November 2010)

One distinct class of band structures, spin gapless semiconductors in which both electrons and holes can be fully spin polarized, has been proposed recently [X. L. Wang, Phys. Rev. Lett. **100**, 156404 (2008)]. Exotic spin-related phenomena and potential applications were predicted for those semiconductors. In the present work, the electronic structures of BN nanoribbons are studied from *ab initio* calculations. Two kinds of spin gapless semiconductors are predicted in the nanoribbons with certain B or N vacancies. The unique bands are found to be independent of the width of the nanoribbons. The appearance of the spin-polarized bands in BN system without traditional magnetic ions is ascribed to dangling-bond states formed near the vacancies. The magnetism induced by B vacancies is found to be stronger than that by N. The magnetism can be understood well through Stoner rule.

DOI: 10.1103/PhysRevB.82.195308 PACS number(s): 73.22.−f, 75.70.Ak, 71.15.Mb

I. INTRODUCTION

Graphene has aroused great interest since its successful experimental isolation in 2004.[1] Graphene has a particular band structure, in which the valence and conduction bands just touch each other at Dirac point, called a gapless semiconductor.[1–3] Many fascinating properties have been discovered in graphene due to the unique bands, such as high-electron mobility, room-temperature quantum hall effect, and half metallicity.[4–6] Besides graphene, some oxides, e.g., $PbPdO_2$,[7] and Hg-based IV-VI compounds, e.g., HgCdTe,[8] are also gapless semiconductors. Since no threshold energy is required to move electrons from valence states to conduction states, one may flexibly tune the properties of the materials by modifying external conditions, saying, optics field, electric field, and impurities etc.[8,9]

Based on gapless semiconductors, the new concept of spin gapless semiconductors (SGS) was proposed, and discussed in doped $PbPdO_2$.[7] In SGS, at least one of the spin channels in the valence bands just touches only one of the spin channels in the conduction bands at the Fermi level (E_F), or vice versa. Four typical kinds of SGS with parabolic or linear dispersion between energy and momentum were defined in Ref. 7. For most kinds of SGS, one invaluable behavior is the appearance of the 100% spin-polarized holes or excited electrons near the E_F, the most desirable property for semiconductors in spintronics. Some remarkable phenomena have been observed experimentally in the SGS materials, containing colossal current-induced electroresistance and giant magnetoresistance effects, etc.[10] Besides the doped $PbPdO_2$, SGS was also found in zigzag graphene nanoribbons, when single-N atoms are substitutionally doped at the edge of the nanoribbons.[11]

BN single layers, the III-V analogs of graphene, have been fabricated in experiments.[12] Some groups began to investigate the properties of the single layer BN nanoribbons by considering different edge decorations, sample sizes, and external fields. For example, the variation in band gaps of BN nanoribbons with their widths, C-doping effect, and Stark effect were studied in Refs. 13–16. Half metallicity was obtained in zigzag BN nanoribbons when an external electrical field was applied or the B edge was hydrogenated.[16,17] In this work, the electronic structures and magnetism of BN nanoribbons with vacancies were studied from density-functional theory (DFT). Some very special band structures were obtained, including spin-polarized semimetals and semiconductors and two kinds of spin gapless semiconductors. They can be rationalized by using relative shift of spin-up and spin-down impurity states near Fermi level. The magnetism in the system was found to be triggered by dangling-bond states near the vacancies. The predicted behaviors provide opportunities for designing spintronic devices with BN nanoribbons as building blocks.

II. METHOD AND MODEL

The calculations were carried out by using a first-principles pseudopotential plane wave method based on DFT. The employed pseudopotentials were generated from the projector-augmented wave method[18] in the local spin density approximation (LSDA) (Ref. 19) as implemented in VASP package.[20] The plane wave cutoff energy was set to 450 eV. Two adjacent nanoribbons are separated by at least 12 Å to avoid interactions between each other. The convergence threshold for energy is 10^{-6} eV. The typical unit cell studied is given in Fig. 1(a). The structure is periodic along the x direction and finite with eight zigzag B-N chains along y direction. In our calculations, all the edge atoms are passivated by H atoms to saturate the dangling bonds in the edge atoms as shown in Fig. 1(a). The symbols of "B1" and "B2," etc in Fig. 1(a) express different B vacancy positions. If there is one B vacancy at site 1 in Fig. 1(a), we denote the system as "6H-V_{B1}." Here the number of H atoms in segmental ribbon which contains only one vacancy is employed to indicate the vacancy concentration. The denotation is analogous for the case of N vacancies. All the structures concerned were fully relaxed in the lattice parameters and the atomic positions. The convergent criterion of the Hellmann-Feynman forces is 0.01 eV/Å. Displacements usually happen for the atoms near the vacancies.[21–23] For example, in the relaxed

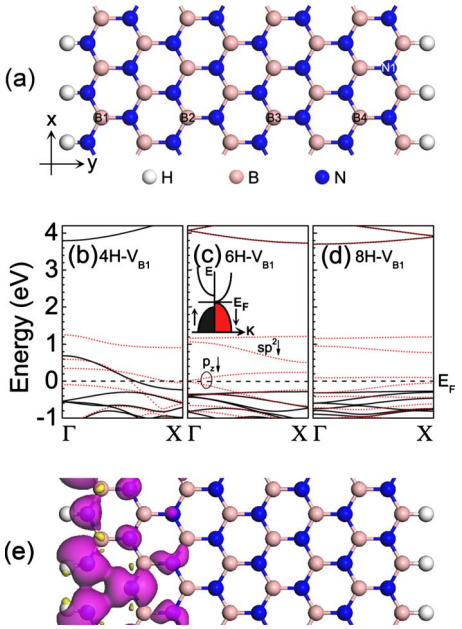

FIG. 1. (Color online) (a) Geometric illustration of one typical zigzag BN nanoribbon studied. The symbols of "B1"-"B4," and "N1" express the different B- or N-vacancy positions considered. (b)–(d) give the band structures of BN nanoribbons with different concentrations of B vacancy at site 1. The black solid and red dotted curves are for spin-up and spin-down channels, respectively. The dashed lines give the E_F. The inset in (c) shows the sketch of SGS obtained. (e) The spatial distribution of the spin difference for 6H-V_{B1}. The magenta (dark gray) density on atoms is for spin-up and yellow (light gray), for spin down.

structure for 6H-V_{B1}, the atoms near the vacancy are pulled away from the position of vacancy. Concretely, the relaxed lengths of the typical B-N bonds close to the B vacancy become 1.410 and 1.397 Å, shorter than the corresponding unrelaxed ones (1.421, and 1.436 Å). The trend is in good agreement with that reported in Ref. 23. The energy of relaxed structure for 6H-V_{B1} is lower than that of the unrelaxed structure by about 237 meV.

III. RESULTS AND DISCUSSION

The band structure of ideal BN nanoribbons without vacancies shown in Fig. 1(a) was studied first. Semiconductor bands with a gap of 3.9 eV was obtained, consistent with the previously published result.[17] No obvious magnetism was found at the zigzag edge atoms. The magnetism, however, can appear when B or N vacancies are formed in the BN nanoribbons. Figures 1(b)–1(d) give the band structures of BN nanoribbons with B vacancies at sites 1 but for different concentrations. The bands for all the three cases are obviously spin-polarized, especially near the E_F, induced directly by the B vacancies injected. With the decrease in the concentration of B vacancy [from Figs. 1(b)–1(d)], the interaction between the adjacent vacancies weakens. This causes reduced energy dispersion of impurity bands, explaining the metal bands formed in 4H-V_{B1} but semiconductor bands in 8H-V_{B1}. For the middle case, 6H-V_{B1}, one kind of SGS appears. As show in Fig. 1(c), the spin-up bands are insulating while the valence and conduction bands for the spin-down channel touch each other at the E_F. Analogous to the concept of half-metal gap defined in half-metal materials,[17] the SGS gap is defined here as the difference between the E_F and topmost occupied spin-up band, about 0.3 eV in Fig. 1(c). To check the stability of the magnetism in 4H-V_{B1}, the total energy of antiferromagnetic state was calculated, 38 meV higher than that of ferromagnetic state. In this kind of SGS, both the conducting electrons and holes are 100% spin polarized. To test if the bands of SGS depend sensitively on the width of the ribbon, we calculated the band structures of the doped ribbons with 4 and 12 zigzag chains in y directions. For both cases, the bands of SGS remained. Since SGS is judged from the state distribution around E_F, which may depends on the employed LSDA in certain systems, it is of importance to check the results beyond the LSDA. Zheng *et al.* employed GW approximation method to study the band structures of BN nanoribbons with the edges passivated or unpassivated by H atoms.[17] They found the results produced from GW are in good agreement with the results from LSDA,[17] indicating LSDA can describe the electronic structures of BN system reasonably.

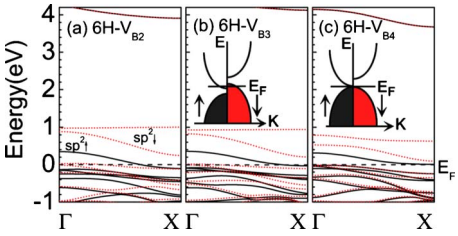

FIG. 2. (Color online) The band structures of BN ribbons with B vacancies at sites 2 (a), 3(b), and 4(c), respectively. The concentration of B vacancies is the same as that in Fig. 1(c). The black solid and red dotted curves are for spin-up and spin-down channels, respectively. The dashed lines in the band structures give the E_F. The insets show the sketches of special bands obtained: (b) spin-polarized semimetals and (c) SGS (another kind).

To understand the magnetism of BN ribbons with B vacancies, we plot the spatial distribution of spin difference in Fig. 1(e) for 6H-V_{B1}. One can see clearly no spin polarization exists at B edge while obvious spin polarization appears at N edge, especially, at the three N atoms nearest to the B vacancy. In the pure BN sheet, the valence bands near the E_F are mainly composed by N p_z electrons.[24] The hybridized states of N s, p_x, and p_y, called sp^2 hereafter, are located at slightly low energy.[24] After B vacancies are injected into the compounds, the three N atoms nearest to the vacancy will have dangling bonds in the ribbon plane. These relatively unstable dangling-bond states (sp^2) are located at higher energy than p_z states for certain spin channel, as shown in Fig. 1(c). It is these sp^2 dangling-bond states that initiate the magnetism in the system.

The band structures with the B vacancy on other sites (B2-B4) are given in Fig. 2. Upon the B vacancy moving from site 1 to 2, the environments of the two N atoms nearest to the vacancy vary significantly, as their bonding to H is changed to B, causing the impurity bands to change. From

TABLE I. The band structure, total magnetic moment per vacancy M (in μ_B), and the energy difference ΔE (in meV) obtained for each case. For the "band" row, "M," "SC," and "SM" express metal, semiconductor, and semimetal bands, respectively. The energy difference is defined as $\Delta E = E_{NM} - E_M$, where E_{NM} and E_M are the total energies for the nonmagnetic and magnetic states in one unit cell, respectively.

	B Vacancy						N Vacancy		
	4H-V_{B1}	6H-V_{B1}	8H-V_{B1}	6H-V_{B2}	6H-V_{B3}	6H-V_{B4}	4H-V_{N1}	4.7H-V_{N1}	6H-V_{N1}
Band	M	SGS	SC	M	SM	SGS	M	SGS	SC
M	1.8	3.0	3.0	1.7	1.5	1.0	0	0.3	1.0
ΔE	153	475	671	152	115	83	0	13	73

Fig. 1(c) to Fig. 2(a), both the spin-down sp^2 and p_z states shift down in the case of site 2 while the spin-up states move up. Consequently, the strength of the spin polarization decreases. As the sp^2 (mainly spin-up) bands cross the E_F, the bands of 6H-V_{B2} become metallic. If the B impurities move further to site 3, the environment of the N nearest to the impurities does not vary much. This is why the bands of Fig. 2(b) are very similar to those in Fig. 2(a), besides the weaker strength of the spin polarization. As shown in Fig. 2(b), one more very special kind of band structure, a spin-polarized semimetal, is formed for 6H-V_{B3}. For 6H-V_{B4} ribbon, another kind of SGS is predicted, in which the spin-up sp^2 bands are located above the E_F. They touch the top of valence bands in energy space [Fig. 2(c)]. For this kind of SGS, only the excited electrons are 100% spin polarized. The spin-down p_z states in Fig. 2 vary little with the vacancy position, which may be ascribed to the orbit distribution, perpendicular to the ribbon plane. They are not as sensitive as the hybridized sp^2 orbitals (along ribbon plane) to the vacancy positions. Thus, the band transitions with the variation in the vacancy position can be ascribed to the relative movements of the spin-up and spin-down sp^2 dangling-bond states on N nearest to the vacancy. With the development of experimental techniques, more advanced methods can be employed to generate nanopatterns in single atomic layers. For example, Bai *et al.*[25] reported to produce periodic nanomeshes in a graphene flake with tunable neck widths through block copolymer lithography. And Rodríguez-Manzo *et al.*[26] showed that lattice defects (vacancies) in carbon nanotubes or graphene can be created by focusing an electron beam in a scanning transmission electron microscope onto a 1 Å spot on the object. Those techniques guarantee the possibility to fabricate the proposed samples currently or in near future.

The band structures for BN nanoribbons containing B vacancies are summarized in Table I. The total magnetic moment per vacancy in each case is also given. It becomes stronger with decreasing concentrations and saturates at 3.0 μ_B for 6H sample, understood by the ideal dangling-bond picture on the three N atoms nearest to the B vacancy. When the B vacancy moves from the N edge gradually to the B edge, the total magnetic moment decreases. This phenomenon is consistent with the moving down of spin-down bands and moving up of spin-up bands in Fig. 2. The decrease in spin polarization can be rationalized by the fact that the localization of N atoms, rich at N edge, is stronger than B atoms, rich at B edge.[24] The trend will also be seen in the following charge contours. An integer magnetic moment in the unit cell is obtained for the bands of SGS or semiconductors, similar to the case in half metals.[27] The energy difference between the nonmagnetic structure and the magnetic structure is given as ΔE in Table I. Positive ΔE means the system with magnetic state has low total energy, indicating magnetic state is stable. The trend of ΔE varying with the concentration and the site of B vacancy is completely the same as the total magnetic moment. For example, higher concentration of B vacancies (from 8H-V_{B1} to 4H-V_{B1}) leads to smaller magnetic moment and lower ΔE. This behavior can be ascribed to the increase in the coupling (small attractive interactions) between the vacancies at high concentration. The localization of the atoms near to the vacancies thus becomes weak, leading to the decrease in the magnetism in the systems. The trend will be explained further by Stoner criterion (Fig. 5).

The effect of N vacancy on the bands of zigzag BN nanoribbons is also studied. The band structures of 4H-V_{N1} and 6H-V_{N1} are depicted in Fig. 3. For 4H-V_{N1}, metallic bands are obtained, in which the bands around E_F and 1–2 eV above the E_F are the N-vacancy states. As in the case of B vacancy, the N-vacancy bands are mainly composed of s, p_x, and p_y states of B atoms nearest to the N vacancy. Compared to 4H-V_{B1}, the obvious difference is no spin polarization in bands for 4H-V_{N1}, explained by the spatial distribution of the charge density. As shown in Figs. 4(a) and 4(b), the spatial extension of the impurity states induced by N vacancies is more extensive than that by B vacancies, which reasonably reflects the fact that N atoms blind electrons more tightly than B atoms do. This trend also illustrates why the magnetism decreases for the BN ribbon, with B vacancy moving from N edge to B edge. However, with the decreasing con-

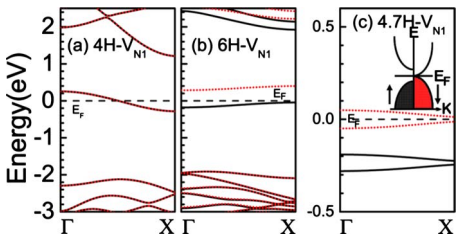

FIG. 3. (Color online) Energy band structures of zigzag BN nanoribbons with N vacancies at different concentrations: (a) 4H-V_{N1}, (b) 6H-V_{N1}, and (c) 4.7H-V_{N1}. The black solid and red dotted curves are for spin-up and spin-down channels, respectively. The dashed lines in the band structures give the E_F. The inset in (c) shows the sketch of SGS obtained.

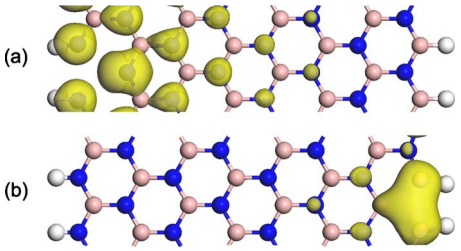

FIG. 4. (Color online) The partial charge densities (yellow or light gray) for (a) 4H-V_{B1} and (b) 4H-V_{N1} in the energy range from −0.4 eV to E_F.

centration of N vacancies, the bands become weakly spin-polarized, as shown in Fig. 3(b). The energy difference between the nonmagnetic and magnetic structures for 6H-V_{N1} (73 meV) is much less than the corresponding case for B vacancies (475 meV). Since the bands change from metals to semiconductors from Fig. 3(a) to Fig. 3(b), some critical bands are expected to appear in between. Therefore, we considered one medium concentration between the cases of Figs. 3(a) and 3(b), the ribbon of 4.7H-V_{N1}, whose bands are given in Fig. 3(c). It is exciting to find a spin gapless semiconductor again, the same kind as in Fig. 1(c). The magnetic moments, band structures, and the energy differences of the BN ribbons with N vacancies are listed in the right side of Table I. As shown in Table I, SGS usually come out between the band structures of metals and semiconductors. This behavior gives a hint to find SGS. Note that in the present work, the electronic structures of BN nanoribbons with vacancies are only studied at $T=0$ K. For a real material, vacancy diffusion may not be avoided due to the thermal effect. It may affect slightly the behaviors of the SGS predicted, like other properties obtained from DFT calculations in semiconductors. Some further thermodynamic investigations will be helpful to the problem.

The magnetism in BN ribbons with B or N vacancies, systems without traditional magnetic ions, can be called d_0 magnetism or *sp* magnetism.[28–30] The mechanism can be understood by using the stoner criterion.[31] For an itinerant electron system, the spin-polarized state is stable if $I_{eff}N(E_F) > 1$, where $N(E_F)$ is the density of one electron states per atom per spin at the Fermi level in the paramagnetic state and I_{eff} is an on-site interaction parameter. The on-site interaction parameter I_{eff} is commonly small in systems with only *s* and *p* valence electrons. Thus, very high density of states (DOS) at the E_F is necessary for magnetism in systems of this kind. The higher and more localized peaks of DOS

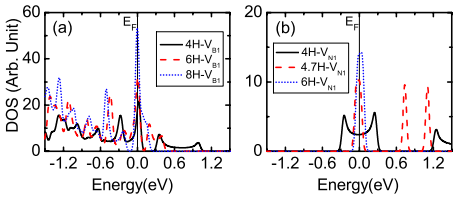

FIG. 5. (Color online) The total DOSs of the nanoribbons with (a) B and (b) N vacancies at different concentrations. The DOSs were calculated without considering spin polarization.

around the E_F will induce larger spin splitting. The DOSs of zigzag BN nanoribbons with B or N vacancies at different concentrations are shown in Fig. 5. There are indeed high peaks of the DOSs at E_F for the all three cases with B vacancies. And the height of the peak increases with the decrease in the concentration of the B vacancy. Since a high peak around E_F is extremely unstable, it finally causes the system spin splitting.[31] For N vacancy, a very short and flat state appears around E_F in the sample of 4H-V_{N1}. Thus, in this case, no spin polarization is triggered.

IV. SUMMARY

By using first-principles calculations, the electronic and magnetic structures of BN nanoribbons with B or N vacancy are studied. Some very special band structures are obtained, including spin-polarized semimetals and semiconductors and two kinds of spin gapless semiconductors. The appearing of those various bands can be explained by the relative shift of the spin-up and spin-down impurity states near Fermi level. The obtained spin gapless semiconductors are found to be insensitive to the width of the nanoribbons. The magnetism observed in the system is ascribed to dangling-bond states formed due to the vacancies. The magnetism induced by B vacancies is stronger than that by N. Those unique and interesting bands achieved in BN nanosystems are full of potential applications in future electronics.

ACKNOWLEDGMENTS

We are grateful to M. Ratner for very helpful discussion. The work was supported by the National Natural Science Foundation of China under Grant No. 10674027, 973-projects under Grants No. 2006CB921300 and No. 2011CB921803, the China Scholarship Council, Fudan High-end Computing Center, and the Chemistry and Materials Research Divisions (MRSEC program) of the NSF and the DOE in USA.

*zyang@fudan.edu.cn

[1] K. S. Novoselov, D. Jiang, F. Schedin, T. J. Booth, V. V. Khotkevich, S. V. Morozov, and A. K. Geim, Science **306**, 666 (2004).

[2] A. K. Geim and K. S. Novoselov, Nature Mater. **6**, 183 (2007).

[3] I. M. Tsidilkovski, in *Electron Spectrum of Gapless Semiconductors*, Springer Series in Solid-State Sciences Vol. 116, edited by K. von Klitzing (Springer, New York, 1996), and references therein.

[4] K. S. Novoselov, A. K. Geim, S. V. Morozov, D. Jiang, Y. Zhang, S. V. Dubonos, I. V. Grigorieva, and A. A. Firsov, Nature (London) **438**, 197 (2005).

[5] Y. Zhang, Y.-W. Tan, H. L. Stormer, and P. Kim, Nature (London) **438**, 201 (2005).
[6] X. Li, X. Wang, L. Zhang, S. Lee, and H. Dai, Science **319**, 1229 (2008).
[7] X. L. Wang, Phys. Rev. Lett. **100**, 156404 (2008).
[8] I. M. Tsidilkovski, G. I. Harus, and N. G. Shelushinina, Adv. Phys. **34**, 43 (1985).
[9] F. Wang, Y. B. Zhang, C. S. Tian, C. Girit, A. Zettl, M. Crommie, and Y. R. Shen, Science **320**, 206 (2008).
[10] X. L. Wang, G. Peleckis, C. Zhang, H. Kimura, and S. X. Dou, Adv. Mater. **21**, 2196 (2009).
[11] Y. F. Li, Z. Zhou, P. W. Shen, and Z. F. Chen, ACS Nano **3**, 1952 (2009).
[12] K. S. Novoselov, D. Jiang, F. Schedin, T. J. Booth, V. V. Morozov, and A. K. Geim, Proc. Natl. Acad. Sci. U.S.A. **102**, 10451 (2005).
[13] A. J. Du, S. C. Smith, and G. Q. Lu, Chem. Phys. Lett. **447**, 181 (2007).
[14] Z. H. Zhang and W. L. Guo, Phys. Rev. B **77**, 075403 (2008).
[15] C. H. Park and S. G. Louie, Nano Lett. **8**, 2200 (2008).
[16] V. Barone and J. E. Peralta, Nano Lett. **8**, 2210 (2008).
[17] F. W. Zheng, G. Zhou, Z. R. Liu, J. Wu, W. H. Duan, B. L. Gu, and S. B. Zhang, Phys. Rev. B **78**, 205415 (2008).
[18] P. E. Blöchl, Phys. Rev. B **50**, 17953 (1994).
[19] J. P. Perdew and A. Zunger, Phys. Rev. B **23**, 5048 (1981).
[20] G. Kresse and D. Joubert, Phys. Rev. B **59**, 1758 (1999).
[21] M. S. Si and D. S. Xue, Phys. Rev. B **75**, 193409 (2007).
[22] M. Topsakal, E. Aktürk, and S. Ciraci, Phys. Rev. B **79**, 115442 (2009).
[23] S. Azevedo, J. R. Kaschny, C. M. C. de Castilho, and F. de Brito Mota, Nanotechnology **18**, 495707 (2007).
[24] R. F. Liu and C. Cheng, Phys. Rev. B **76**, 014405 (2007).
[25] J. Bai, X. Zhong, S. Jiang, Y. Huang, and X. Duan, Nat. Nanotechnol. **5**, 190 (2010).
[26] J. A. Rodríguez-Manzo, O. Cretu, and F. Banhart, ACS Nano **4**, 3422 (2010).
[27] Z. Q. Yang, L. Ye, and X. Xie, Phys. Rev. B **59**, 7051 (1999).
[28] J. A. Chan, Stephan Lany, and Alex Zunger, Phys. Rev. Lett. **103**, 016404 (2009).
[29] C. Das Pemmaraju and S. Sanvito, Phys. Rev. Lett. **94**, 217205 (2005).
[30] J. M. D. Coey, M. Venkatesan, P. Stamenov, C. B. Fitzgerald, and L. S. Dorneles, Phys. Rev. B **72**, 024450 (2005).
[31] E. C. Stoner, Proc. R. Soc. London, Ser. A **154**, 656 (1936); **165**, 372 (1938).